

SUBWAVELENGTH LOCALISATION IN DISORDERED SYSTEMS

HABIB AMMARI , SILVIO BARANDUN , AND ALEXANDER UHLMANN 

ABSTRACT. We consider disordered finite systems of subwavelength resonators where the disorder is in the spatial arrangement of the resonators and their material parameters are perturbed randomly. We elucidate the mechanism of wave localisation in such systems. To do so, we employ the capacitance matrix formalism, make precise the notions of bandgap and localised eigenmodes, study their stabilities with respect to fluctuations in the system, and highlight the importance of defect hybridisation and level repulsion in creating localised eigenmodes for a given arrangement of the resonators by randomly changing their material parameters. We also introduce a method of localised eigenmode prediction based on the discrete Green function of the disordered system of resonators and show the existence of *hybridised bound eigenmodes* in disordered systems where local translation invariance is broken.

Keywords. Disordered system, subwavelength localisation, delocalisation, bandgap, hybridised bound eigenmode, defect eigenmode.

AMS Subject classifications. 35J05, 35C20, 35P20.

1. Introduction

A subwavelength resonator is a highly contrasted bounded inclusion. The high contrast property gives rise to subwavelength resonances, which are frequencies at which the resonator strongly interacts with incident waves whose wavelengths can be larger by several orders of magnitude [10]. A typical example in acoustics of a subwavelength resonator is an air bubble in water, where the associated subwavelength resonance is called Minnaert resonance [14, 39].

Systems of subwavelength resonators can be used to achieve wave localisation at subwavelength scales [18, 19, 32, 33, 34, 35, 37, 51]. From [14, 24], we know that their spectral properties are (approximately in terms of the high contrast material parameter) described in one and three dimensions by the product of two matrices, V and C . V is a diagonal matrix where its diagonal terms are the material parameters of each resonator and C is the so-called *capacitance matrix* which contains only geometric information on the system of resonators. In the two-dimensional case, a similar capacitance matrix approximation holds. However, it is less elegant than those in one or three dimensions considered here [10, 11].

We let $D := \cup_{i=1}^N D_i$ be a system of N resonators. To fix ideas, we consider an acoustic setting and denote by v_i, ρ_i, κ_i , the wave speed, the density, and the bulk modulus of the resonator D_i . We let v, ρ, κ be the material parameters associated with the background medium. We also let $\delta_i = \rho_i/\rho$ be the contrast between the densities inside and outside the resonator D_i and assume that for $i = 1, \dots, N$, $\delta_i = \mathcal{O}(\delta)$ with δ being small while the wave speeds v_i are all of order v .

The entry C_{ij} of the so-called *generalised capacitance matrix*, $\mathcal{C} := VC$, describes the interaction between the resonators D_i and D_j . The matrix V reads

$$V := \begin{pmatrix} \frac{v_1^2 \delta_1}{|D_1|} & & \\ & \ddots & \\ & & \frac{v_N^2 \delta_N}{|D_N|} \end{pmatrix}, \quad (1.1)$$

where $|D_i|, i = 1, \dots, N$, denotes the volume (or the length in dimension one) of D_i , while C_{ij} is given by

$$C_{ij} := - \int_{\partial D_i} \frac{\partial \phi_j}{\partial \nu} d\sigma, \quad (1.2)$$

where ν is the outward at the boundary ∂D_i of D_i and ϕ_j is the solution to the Laplace equation outside D with the boundary condition $\phi_j = \delta_{ij}$ on ∂D_i , which behaves as $\mathcal{O}(1/|x|)$ (resp. as $\mathcal{O}(1)$) in three (resp. one) dimensions as $|x| \rightarrow +\infty$; see [10, 24]. From [10, 11], we know that the system exhibits N subwavelength resonant frequencies (with non-negative real parts) in the subwavelength regime $\delta \rightarrow 0$, approximated in leading order by

$$\omega_i(\delta) = \sqrt{\lambda_i} + \mathcal{O}(\delta), \quad 1 \leq i \leq N, \quad (1.3)$$

where the λ_i 's denote the eigenvalues of the generalised capacitance matrix \mathcal{C} . Moreover, propagating the eigenvectors of \mathcal{C} yields their associated eigenmodes.

When the system of resonators is periodic (*i.e.*, is translationally periodic in one, two, or three dimensions), the generalised capacitance matrix has, depending on the number of resonators per unit cell, a Toeplitz or block Toeplitz structure perturbed at its edges; see [4, 10].

The infinitely periodic case is then described by a Laurent operator where quasiperiodic Bloch solutions and their respective band functions give a full description of the essential spectrum. For increasing numbers of unit cells, pointwise convergence of the eigenvalues of the finite system C to the essential spectrum of the corresponding Laurent operator was proved in [13]. In other terms, any eigenvalue/eigenvector of the quasiperiodic capacitance matrix (associated with infinite structure) can be approximated by eigenvalues/eigenvectors of C . The converse is in general not true because of the edge effect, which is the greatest on eigenfrequencies within the first radiation continuum (*i.e.*, around the origin of the Brillouin zone). The existence of a bandgap for such a Laurent operator shows the existence of a bandgap for C when its size (the number N of resonators) is large enough. Moreover, it was shown in [9] that defect eigenmodes in infinite systems introduced by perturbing the material parameters of a fixed number of resonators (*i.e.*, taking V differing from the identity matrix on a fixed number of diagonal entries) have corresponding eigenmodes in finite systems which converge as the size of the system increases.

On the one hand, in [13], the truncated Floquet–Bloch transform, a key tool to approximate the spectral properties of large finite subwavelength resonator systems, has been introduced. It gives a concrete way to associate bandgaps and localised eigenmodes to systems of resonators that may be finite periodic or aperiodic (such as Su–Schrieffer–Heeger (SSH) and dislocated chains). The main idea is that, when the size of the finite structure is sufficiently large, the structure's eigenmodes are approximately a linear combination of Bloch eigenmodes of the corresponding infinite structure. To compare the discrete eigenvalues of the finite structure to the continuous spectrum of the infinite periodic structure, one can reverse engineer the appropriate quasiperiodicities corresponding to these Bloch eigenmodes, taking into account the symmetries in the problem. The discrete band function and defect eigenmode calculations in [9, 13] provide a notion of how an eigenmode of the finite problem is approximated either by Bloch eigenmodes (delocalised eigenmodes) or defect modes (localised eigenmodes, corresponding to defect eigenfrequencies inside a bandgap) of the infinite structure. We refer to [7] for the mathematical foundations of the Floquet–Bloch transform.

On the other hand, in [8] it was shown that the scattering of waves in three dimensions by periodic systems of resonators where their material parameters are perturbed randomly (*i.e.*, entries of V are perturbed randomly) reproduces the characteristic features of Anderson localisation and illustrates for the first time strong subwavelength localisation in random systems with long-range interactions. By Anderson localisation, we mean an increase in both the degree of localisation and the number of localised eigenmodes on average when we increase the random perturbation of the system. Moreover, it was also shown in [8] that the hybridisation of subwavelength eigenmodes is responsible for both the repulsion of eigenfrequencies as well as the phase transition, at which point eigenmode symmetries swap and very strong localisation is possible. The localised eigenmodes were characterised in terms of Laurent operators and the generalised capacitance matrix \mathcal{C} .

All of the recalled results obtained in the subwavelength regime heavily rely on the translation invariance properties of the system of resonators (or analogously the almost Toeplitz or block Toeplitz structure of C) together with the use of Floquet–Bloch theory for the analysis of the spectral properties of the corresponding infinite structure.

The aim of this work is to show that similar results and wave localisation mechanisms can be obtained in disordered systems. Our work can be seen as a first attempt to construct a consistent picture of how wave localisation occurs at subwavelength scales in disordered systems of subwavelength resonators. By disordered, we mean systems that are not translationally invariant. It is worth emphasising that here the disorder is in the spatial distribution of the resonators. We will show that localised eigenmodes can be created in these systems, under some conditions on the spatial distribution of the resonators, by randomly varying the material parameters of the resonators. To do so, we need to introduce the notions of bandgap and defect midgap eigenmode. Recall first from [11] that in dimension three the matrix C corresponding to a system of subwavelength resonators is a nonsingular real symmetric M-matrix, *i.e.*, it is diagonal dominant, all of its off-diagonal terms are negative, and its C_{ij} entry decays as the distance between the resonators D_i and D_j for large enough $|i - j|$, showing long-range interactions in the resonator’s system; see [26, 41, 42, 48]. Recall also that in dimension one the matrix C is a real tridiagonal symmetric matrix and 0 is an eigenvalue of C with the associated eigenvector given by $(1, \dots, 1)^\top$. Here, the superscript \top denotes the transpose.

Our first goal is to introduce the notions of bandgap and midgap eigenvalue for C and/or \mathcal{C} and to construct several disordered systems that exhibit these phenomena. Then, assuming that C exhibits a bandgap, we show that by randomly perturbing the material parameters of the resonators, as in [8], we can evolve localised eigenmodes from extended eigenmodes and study how the localisation length and the portion of localised eigenmodes in the system vary as the amount of disorder is increased. By localised eigenmode, we mean an eigenvector $v = (v_1, \dots, v_N)^\top$ of C or \mathcal{C} such that $\|v\|_\infty / \|v\|_2 := \max_i |v_i| / (\sum_i |v_i|^2)^{1/2}$ is close to 1.

As said above, while for finite periodic structures the associated eigenmodes are approximately linear combinations of Bloch eigenmodes of the corresponding infinite structure, this fact is in general not true for disordered systems. However, as first observed by Edwards and Thouless [23], if we repeat the disordered structure periodically, then a localised eigenmode must be an eigenmode of the obtained periodic structure for any quasiperiodicity. In other words, by looking at the sensitivity of the eigenmodes to the quasiperiodic boundary conditions, we can distinguish between localised and delocalised eigenmodes. While the delocalised eigenmodes of the disordered structure are sensitive to the periodisation of the structure, the localised ones are very insensitive. Conversely, if a Bloch band of the obtained periodic structure is flat (*i.e.*, independent of the quasiperiodicity), then such an eigenfrequency corresponds either to a localised eigenmode or to one of the edges of the bandgap. By this reasoning, we introduce natural notions of localisation and bandgap in disordered structures. The strategy is as follows: by periodising the disordered finite structure and looking at the variation of the eigenfrequencies of the infinitely periodic structure as a function of the quasiperiodicity we can detect band edges and consequently also the existence of a bandgap

in the distribution of the eigenvalues of the capacitance matrix C . We may also detect localised eigenmodes inside such bandgaps. We recall that the quasiperiodic eigenfrequencies of the infinite system are obtained as the eigenvalues of the *quasiperiodic capacitance matrix* C^α defined in (2.1); see [10, 11]. A remarkable finding is that, depending on the disorder, “hybridised bound eigenfrequencies” may exist. These eigenfrequencies do correspond to *quite* localised eigenmodes (they are less localised than those in the bandgap) and accumulate as the number of resonators increases while the number of localised eigenmodes stays finite. Such “hybridised bound eigenmodes” do not exist in periodic systems of subwavelength resonators. They also don’t occur in dislocated chains of resonators or finite chains of SSH type. In both cases, the structure is composed of two half-periodic systems having the same band structure. In some sense, to display such hybridised bound eigenmodes, disordered systems must differ significantly from periodic ones and break even local translation invariance. Hybridised bound eigenmodes can then occur for resonant frequencies which are partially supported in these systems whereas defect modes that are supported nowhere are fully localised.

Moreover, in this paper, we show that starting, as in the finite periodic case, from a disordered structure exhibiting a bandgap, we can introduce localised eigenmodes by perturbing the material parameters of some resonators. We reproduce for the first time a transition between localisation and delocalisation phases for disordered systems of subwavelength resonators. Furthermore, we implement Thouless’ criterion [45] for disordered subwavelength systems of resonators.

In this work, we focus on one-dimensional models for the simulations to simplify the computations. Nevertheless, there is no reason to expect different results in three dimensions, as our methods are based on the properties of eigenvectors and not on the structure of the involved matrices.

Finally, it is worth mentioning that our results in this paper generalise those obtained on the localisation of electrons in disordered lattices [1, 38, 40, 46] to classical systems of subwavelength resonators where, despite being in the low-frequency regime, the subwavelength resonances of the system interact strongly with the disorder. For similar results on the continuous Schrödinger model, we refer the reader to [28] and the references therein. It should be noticed that the localisation mechanism for the continuous Schrödinger model, which is due to potential wells is fundamentally different from the discrete models studied here. To our knowledge, the landscape localisation theory [16, 25, 36] is one of the most intriguing ways to detect localised eigenfunctions in the continuous Schrödinger model. An effective potential (known as a landscape function) finely governs the confinement of the localised eigenfunctions. In this picture, the boundaries of the localisation subregions for low-energy eigenfunctions correspond to the barriers of this effective potential, and the long-range exponential decay characteristic of localisation is explained as the consequence of multiple tunnelling in the dense network of barriers created by this effective potential. In [20], a landscape theory for the generalised capacitance matrix is developed and used to predict wave localisation positions in random and aperiodic systems of subwavelength resonators. In [26], it is shown that the landscape localisation theory is valid for all M-matrices.

The paper is organised as follows. In Section 2 we introduce the notion of bandgap for disordered systems and show how to identify mobility edges, localised eigenmodes, and hybridised bound eigenmodes. In Section 4, by randomly perturbing the material parameters of the resonators, we reproduce Anderson localisation features in disordered systems, which can be understood by considering the simple phenomena of *hybridisation* and *level repulsion*. In Section 5 we investigate the stability and behaviour of the bandgaps and hybridised bound eigenfrequencies under random perturbations of the material parameters of all resonators. In Section 6, we compare the performance of the landscape function for the detection of localised eigenmodes in perturbed periodic systems with that in disordered systems when hybridised eigenmodes occur. We also show that the behavior of the fractal dimension related the eigenmodes of randomly perturbed disordered systems can be used to identify the mobility

edges even in the presence of hybridised eigenmodes. Finally, in Section 7 we summarise our main contributions in this paper and formulate some open questions.

2. Bandgaps and band variation

It is well known that the subwavelength part of the spectrum of periodic systems of subwavelength resonators where there are N resonators per unit cell is given by the union of the first N band functions as a result of Floquet–Bloch’s theorem [10, 11, 15]. Recent results obtained in [7, 13] have shown that the subwavelength part of the spectrum of the infinite system can be approximated by the subwavelength eigenfrequencies associated with large size, finite systems. Furthermore, the boundary of the essential spectrum gives the mobility edges discriminating between localised and delocalised eigenmodes.

This theory does not apply to disordered systems, but the distinction and prediction of whether a frequency corresponds to a localised or a delocalised eigenmode are still highly relevant. To do that, we generalise the idea introduced in [23] where the sensitivity of the eigenvalues to the choice of periodic or antiperiodic boundary conditions was used as a criterion for localisation, as follows. The main difference between a localised and a delocalised eigenmode is its magnitude at the edges of the system: While a localised eigenmode is *exponentially* small at the edges, a delocalised eigenmode is proportional to a constant there. Consequently, localised eigenmodes are not sensitive to quasiperiodic boundary conditions, while delocalised eigenmodes are. It is therefore natural to consider the system with quasiperiodic boundary conditions at its edges. Denote by $\alpha \mapsto \omega_i^\alpha$ the i^{th} Bloch band function of the system.

We consider three families of disordered systems:

SSH: Inspired by the SSH model, its quantum-mechanical analogue, this model is composed of two periodic systems with different unit cells joined together. In [5], this system is studied in wave physics in the subwavelength regime;

Dislocated: This model is composed of an array of dimers, one of which gets *dislocated* by increasing the intra-resonator distance. We point to [12] for a study of this model;

Disordered blocks: This model, which actually generalises the other two, consists of a random arrangement of fixed blocks of resonators (dimer blocks and monomer blocks), with known band structure. The disordered block systems considered in this paper will always consist of two distinct building blocks, which are randomly sampled to generate an arbitrarily large disordered system. The behaviour and theory of this class of systems will be further discussed in Section 3.

The family of systems consisting of disordered blocks is more strongly disordered than both the SSH and dislocated system, as even local translation invariance is violated. The eigenmodes are thus no longer given (at least locally) by Bloch eigenmodes, making it impossible to obtain any dispersion relation. Consequently, numerical methods such as the truncated Floquet–Bloch transform, which allows the recovery of the band structure for the SSH and dislocated systems [7], fail to recover anything in the disordered block case.

However, while strongly disordered systems might no longer exhibit the full band structure of their periodic counterparts, we can still observe the familiar notions of band regions and bandgaps.

2.1. Band variation and flat bands

In Figure 1, we show the Bloch band functions for a (A) periodic, (B) SSH, (C) dislocated, and (D) disordered block structure, obtained by imposing quasiperiodic boundary conditions on the respective finite systems. This corresponds to computing the eigenvalues of the quasiperiodic capacitance matrix $C^\alpha : (C_{ij}^\alpha)$ defined analogously to (1.2) by

$$C_{ij}^\alpha := - \int_{\partial D_i} \frac{\partial \phi_j^\alpha}{\partial \nu} d\sigma, \quad (2.1)$$

for $i, j = 1, \dots, N$ (with N being the number of resonators in the disordered system). Here, ϕ_j^α is the solution to the Laplace equation in cell Y containing the set of resonators D with the boundary condition $\phi_j^\alpha = \delta_{ij}$ on ∂D_i , which are quasiperiodic with quasiperiodicity α in the Brillouin zone Y^* associated with Y (i.e., such that $e^{-i\alpha \cdot x} \phi_j^\alpha(x)$ is periodic); see [4, 10]. The N band functions of the system are then given by the Bloch band functions $\alpha \in Y^* \mapsto \omega_p(\alpha)$ mapping a quasiperiodicity α in the Brillouin zone to the p^{th} eigenvalue of C^α .

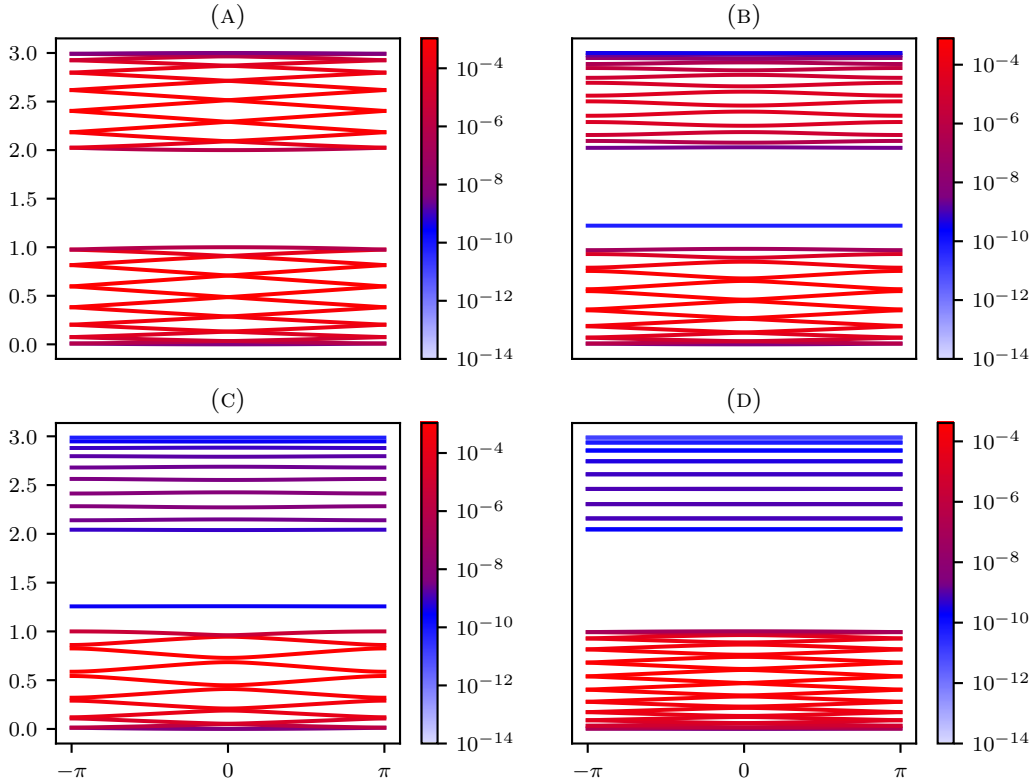


FIGURE 1. The band functions when imposing quasiperiodic boundary conditions to a (A) periodic, (B) SSH, (C) dislocated, and (D) random block system. For each band the colour indicates its variation. There is an obvious bandgap given by the interval $(1, 2)$. At the edges of this gap the variation is lower. The systems (B) and (C) have a defect midgap eigenmode (in light blue) while system (D) has an accumulation of near-to-zero-variance bands.

For any eigenvalue of C we can then calculate the variation of the corresponding band function as an analogue of Thouless' energy [23, 46] in wave physics in the subwavelength regime. Observing Figure 1 we remark the following:

- (i) In all cases there is a rigorous or intuitive idea of what a bandgap for these structures is: the interval $(1, 2)$;
- (ii) As expected, defect “bandgap” frequencies associated to localised eigenmodes have an essentially flat Bloch band function reflecting their insensitivity to boundary conditions;
- (iii) The closer the Bloch band functions are to the bandgap, the flatter they are;
- (iv) Flat bands need not be isolated and may appear in dense regions.

Physically, a structure cannot have a perfectly flat Bloch band function, as Floquet–Bloch’s theorem would then imply a non-empty point spectrum, which is impossible because of the translation invariance property of the system. Nevertheless, Figure 1(B–C) shows that numerically flat bands can be identified with localised eigenmodes.

To distinguish which bands should be considered flat, we suggest comparing their variations with that of the lowest band function. This approach has several advantages. In one dimension the lowest band function is guaranteed to be associated to a delocalised eigenmode, whereas in all dimensions it lays the edge of a band. Furthermore, the variation of the Bloch band functions strongly depends on the size of the system, compared with other variations cancelling this dependence.

2.2. Localisation and hybridised bound eigenmodes

A natural question that arises at this point is whether or not a low band function variation also indicates a high localisation. This is shown to be true in Figure 2 for all four cases presented in Figure 1. The clear clustering shows that the variation of the Bloch band function is an accurate proxy for localisation.

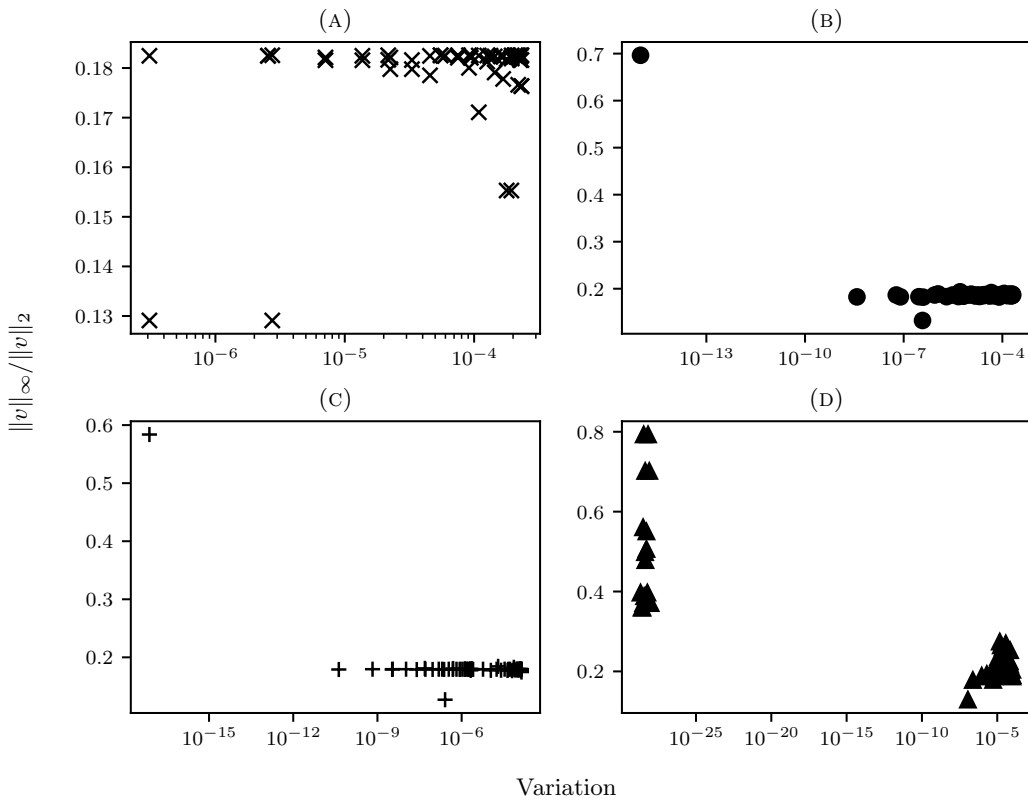


FIGURE 2. Variation of the Bloch band function $\alpha \mapsto \omega_i^\alpha$ versus localisation degree of v_i . Here (A) – (D) refer to the same systems as in Figure 1. Except for (A), which has no localised eigenmodes, the clear clustering shows that the variation of the Bloch band function is an excellent mean to identify localised eigenmodes.

Figure 1(D) shows a region — the interval (2, 3) — which is filled out by essentially flat band functions. In Figure 2(D) it can be seen that even though these eigenmodes do not lie in the bandgap, they are nevertheless quite localised and exhibit very low band function variation. We classify them as *hybridised bound eigenmodes* as they are distinct from

both extended eigenmodes in the band and strongly localised eigenmodes in the bandgap. Furthermore, one notices that for large systems of the same kind, eigenvalues accumulate in this region but the corresponding eigenvectors are localised. This argument would suggest the existence of eigenvalues embedded in the essential spectrum for the corresponding infinite structure. As they appear only in strongly disordered systems as opposed to periodic (or locally perturbed periodic) systems, their existence seems to depend on the violation of local translation invariance.

2.3. Mobility edges and bandgaps

In all four systems of Figure 1, we observe that the regions of high band variation, are flanked by more flat bands at the edges. Thouless' theory of localisation thus also applies to wave physics in the subwavelength regime: Regions of high band variation correspond to *pass bands* and are flanked by a *mobility edge*, which can be detected by using the band variation. In strongly disordered systems, where even local translation invariance is broken, hybridised bound eigenfrequencies may accumulate into regions resembling pass bands. Although these hybridised bound eigenfrequencies all have comparatively low band variation, it is still significantly higher than that of midgap eigenfrequencies and goes down towards the region edges, suggesting a similar mobility edge transition as in the pass band case.

Outside of pass bands and hybridisation regions, we find only strongly localised, isolated midgap eigenmodes induced by defects. Thus, these regions are natural candidates for *bandgaps* in disordered systems of subwavelength resonators. We can identify them as the gaps between regions of eigenvalues, flanked by flat bands indicating mobility edges.

3. Block disordered systems

Systems of randomly sampled resonator blocks, as illustrated in Figure 1 and Figure 4 turn out to be rich models of disordered systems in one dimension as they are amenable to analysis using a powerful propagation matrix approach. We will find a deep agreement between the notions introduced in the previous subsection and the propagation matrices of the constituent resonator blocks.

3.1. Construction

We shall begin by giving a more thorough account of the construction of block disordered systems to enable further analysis later on: Subwavelength block disordered systems are an array of subwavelength resonators $\mathcal{D} = \bigcup_{i=1}^M B_i$ consisting of M blocks of resonators B_i sampled randomly and arranged on a line.

Note that a single resonator block may contain more than one resonator, in particular two for a dimer block. We denote M the total number of sampled blocks and N the total number of resonators. Consequently, we always have $M \leq N$.

EXAMPLE 3.1. A simple but rich disordered system is obtained by sampling from two blocks S and D with probability p_S and p_D , respectively. S denotes a single resonator block with $l = s = 2$ and D a dimer resonator block D with $l_1 = l_2 = 1$ and $s_1 = 1, s_2 = 2$. A single example realisation with $M = 14$ of this system could then be described by the chain

$$SSSSDSSSSSDSSS \quad \text{or} \quad S^4DS^5DS^3,$$

where S^k and D^k denote k repetitions of the single or dimer block, respectively. In Figure 3 another realisation with chain SDS is illustrated.

In this paper, we will only consider blocks sampled independently from a finite collection (that is, of size two) of blocks. A crucial consequence of this kind of sampling is that as the number of sampled blocks M goes to infinity, any local arrangement of blocks must occur infinitely often almost surely.

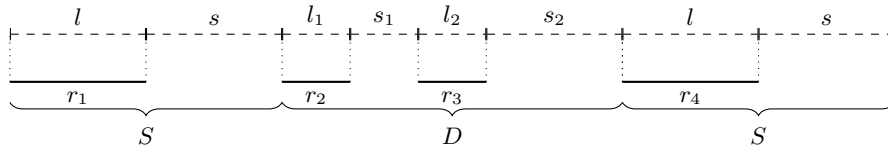


FIGURE 3. A block disordered system consisting of two single resonator blocks S and a dimer block D arranged in a chain as SDS . It thus consists of $M = 3$ blocks and $N = 4$ resonators r_1, \dots, r_4 in total.

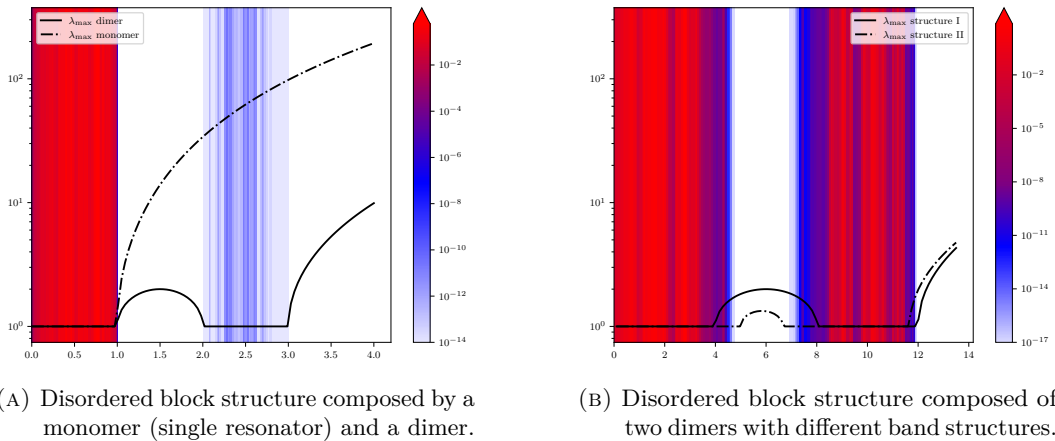


FIGURE 4. Comparison of propagation matrix approach (via its greatest eigenvalue, as lines in the plots) and the band function variation (coloured vertical lines in the plots). Where there are no such lines, the density of eigenmodes is zero. One observes the richness in behaviours due to the possible combinations of in/out of band regions for both structures and the consequent existence of delocalised, hybridised bound, and localised eigenmodes. For each system $M = 100$ blocks were sampled randomly.

3.2. Propagation matrix

The theory of propagation of waves in one-dimensional disordered systems has a long tradition dating back to Saxon and Hutner [44]. We refer in particular to [29, 30] and their theory based on the propagation matrix using Moebius transformations. This approach identifies a frequency in a bandgap if the largest eigenvalue ξ_{\max} of the corresponding total propagation matrix has a magnitude larger than one. The results obtained in this framework are mostly limited to [29, Theorem II] which only partially characterises the resulting band structure. They show that, in a system composed of various blocks, the intersection of the bandgaps of the single blocks must be part of the bandgap of the total system (if certain mixing conditions are met).

In the subwavelength regime the propagation matrix $P_{l,s}(\lambda)$ for a single resonator of length l and spacing s to the subsequent resonator can be formulated as

$$\begin{pmatrix} u(x+l+s) \\ u'(x+l+s) \end{pmatrix} = \underbrace{\begin{pmatrix} 1-ls\lambda & s \\ -l\lambda & 1 \end{pmatrix}}_{P_{l,s}(\lambda):=} \begin{pmatrix} u(x) \\ u'(x) \end{pmatrix} + \mathcal{O}(\delta), \quad (3.1)$$

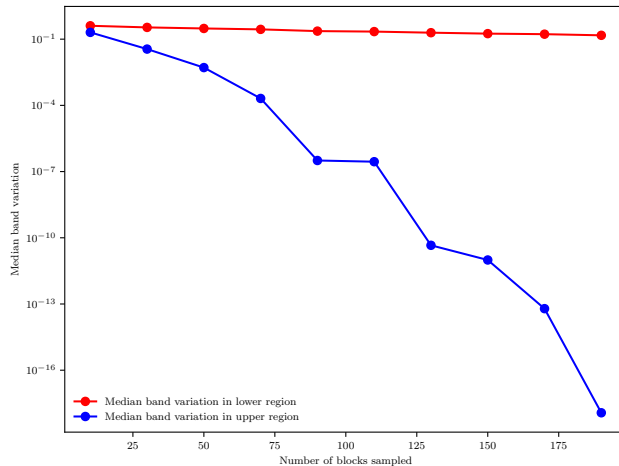


FIGURE 5. Median band variation in the lower spectral region $([0, 1])$ corresponding to the pass band and the upper spectral region $([2, 3])$ corresponding to the hybridisation region as a function of the number of blocks sampled M . We consider disordered systems as in Example 3.1 with $M = 10$ up until $M = 200$ blocks sampled and a high concentration of dimers $p_D = 0.9$. The results are averaged over 100 independent realisations of the disordered system.

where δ is the contrast parameter and the frequency is given by $\omega = \sqrt{\lambda}$. Propagation matrices for blocks consisting of multiple individual resonators can then be obtained by multiplying the constituent single resonator propagation matrices.

In Figure 4 we can then see [29, Theorem II] at work, as in the common bandgaps of the constituent blocks (*i.e.* when $\xi_{\max} > 1$ for all blocks) the density of eigenmodes is zero. However, our method for identifying mobility edges, outlined in the previous subsection, allows us to obtain a richer classification. In Figure 4, we see that using the variation of the Bloch band functions, we not only recover the *entire* bandgap but also identify hybridised bound eigenmodes, which are not covered by propagation matrix theory. In particular, for systems consisting of generic arrangements of resonator blocks (and observing the mixing conditions from [29, Theorem II]), we observe the following complete description of their spectral regions when applying the criteria from the previous subsection: For a block disordered system, a frequency lies in the

Band: if and only if it is in the band of all constituent blocks;

Bandgap: if and only if it is in the bandgap of all constituent blocks;

Hybridisation region: otherwise.

In the bandgap the density of eigenmodes is zero and only defect modes can occur, while both the band and hybridisation regions support resonant modes. However, by comparing their band variations, we can distinguish these modes even without knowledge of the underlying block structure. Figure 5 illustrates that while for eigenvalues in the pass band the band variation remains unchanged as the number of blocks M increases, for eigenvalues in the hybridisation region the band variation decreases exponentially. These results are in line with the intuition that the distinction between pass band, band gap, and hybridisation regions, which is only truly sharp in the infinite limit, becomes sharper as the system size is increased, and is thus sensible for large finite systems.

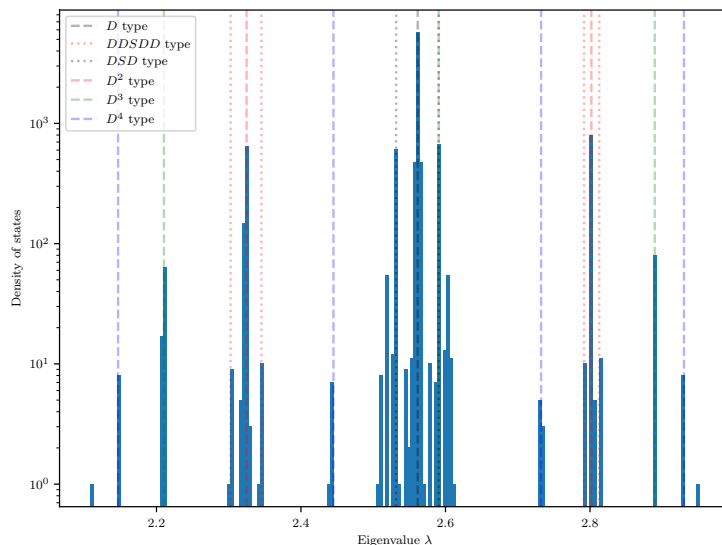


FIGURE 6. Density of eigenmodes in the upper spectral region $[2, 3]$ for the disordered system as in Example 3.1 with a low concentration of dimers ($p_D = 0.1$) and $M = 10^5$ block sampled. The vertical dashed lines denote various types of simple dimer defect modes.

3.3. Fractal density of eigenmodes

As outlined in the previous subsection, the density of eigenmodes of disordered systems can be divided into three types of regions: band regions where the density is nonzero and the corresponding eigenmodes are delocalised, gaps where the density is zero and hybridisation regions which also exhibit a nonzero spectral density.

In this subsection, we aim to better understand the density of eigenmodes in these hybridisation regions as well as the localisation behaviour of the corresponding eigenmodes.

As an illustrative example, we shall again consider disordered systems as in Example 3.1 but with a low density of dimer blocks, namely $p_D = 0.1$, since the fundamental mechanisms at work are most plainly visible in this regime. In Figure 6 we can see that in this regime the density of eigenmodes in the hybridisation region is of fractal nature. In line with [22], there is a clear explanation for this phenomenon: At low dimer density $p_D = 0.1$, the dimers that occur can be seen as defects in an array of identical single resonator blocks. These defect modes can be calculated by taking the defect and attaching an infinite number of single resonators to both sides, *i.e.* $S^\infty DS^\infty$, $S^\infty DDS^\infty$, $S^\infty DS DS^\infty$ and so on. Now, if these defect modes lie in the band gap of the single resonator (which they do for the dimers under consideration), attaching these single resonators amounts to imposing exponentially decaying boundary conditions.

We now turn our attention back to the arbitrarily large disordered system with arbitrarily many “dimer defects” as a consequence. Each dimer block introduces defect modes in the hybridisation region, and because these defect modes are exponentially decaying when passing through single resonators, they barely interact with other defects causing the actual eigenvalue introduced to be exponentially close to the eigenvalue of the defect mode. This can be observed in Figure 6 where the peaks in probability density perfectly align with the defect modes. The fractal nature of the density of eigenmodes is then explained by the relative probabilities of the defect types. For example, a defect of type D occurs roughly 10 times as often as a defect of time DD because $p_D = 0.1$. However, because the defect modes for D, D^2, D^3, \dots type defects form a dense subset of $[2, 3]$, the density of eigenmodes

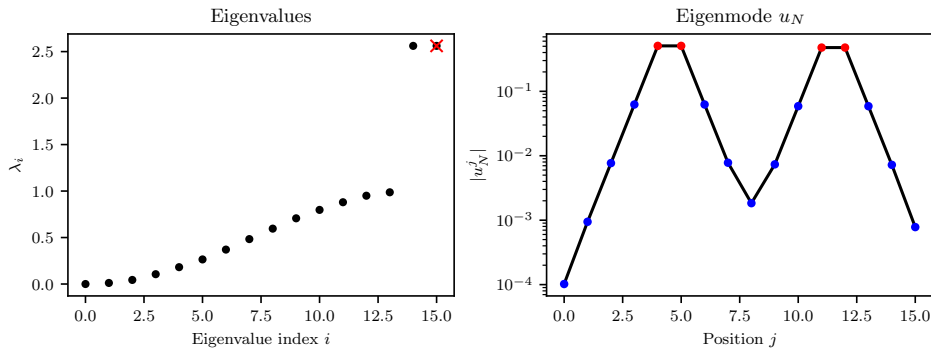


FIGURE 7. Disordered system as in Example 3.1 with chain $S^4DS^5DS^3$. **Left:** Eigenvalues of the disordered system. **Right:** Eigenmode belonging to the marked eigenvalue on the left. Sites corresponding to single resonators or dimers are marked blue or red respectively. We can see that the hybridised bound eigenmode becomes colocated at the two dimers.

of the disordered system will also become nonzero in a dense subset of $[2, 3]$ as the number of blocks sampled M increases.

As the density of dimers increases, the mechanism remains the same. However, the stronger hybridisation of the dimer eigenmodes causes the defect mode peaks to be less pronounced.

3.4. Localisation of hybridised bound eigenmodes

After the density of eigenmodes we now turn our attention to the hybridised bound eigenmodes. In line with similar systems of disordered nature, we might expect some Anderson localisation to occur, causing the hybridised bound eigenmodes to be exponentially localised. This would be in line with what the early numerical experiments indicated; see, for instance, [23].

However, there exists a crucial difference in our setting that prevents this kind of localisation. Due to independent sampling from a finite collection of blocks, any finite subsection must repeat infinitely often almost surely in the infinite limit. As a consequence, each “defect mode” induced by a local structure (*i.e.*, a single dimer surrounded by some single resonators) must occur infinitely often, and while they interact only exponentially weakly, they still interact. This causes a hybridisation of exponentially localised defect modes into delocalised modes, located at an infinite number of sites and exponentially decaying in between. Figure 7 shows a disordered system containing two dimers separated by 5 single resonators. We can see that each of the dimers introduces a hybridised bound eigenmode with almost identical eigenvalue. However, the eigenmodes hybridise and become located around both dimers equally.

EXAMPLE 3.2. For a simple model of this behaviour, we can consider the chain DS^dD of two dimers, separated by d single resonators. By exploiting the spatial symmetry and following a similar argument as in [6, Appendix B], we can show that there exist two dimer modes, one of which is spatially symmetric, while the other is anti-symmetric about the middle of the resonator array. In contrast, numerical simulations would suggest exponentially localised eigenmodes already for $d \approx 15$ separating single resonators, illustrating the numerical difficulties these hybridised bound eigenmodes present.

4. Defect frequencies

Having identified a method of creating strongly disordered systems with well-defined bands and bandgaps we are now in a position to investigate localised defect eigenmodes in the disordered setting. There are multiple strategies on how to modify a periodic structure of subwavelength resonators with a bandgap to support localised defect eigenmodes [10, 11]. In this section, we consider one of these — the most suited for disordered systems — and show that it generates localised eigenmodes in disordered structures.

In this section, we consider a structure of any type known to have a bandgap in the sense of Section 2 and seek to slightly modify the system to get (at least) one localised eigenmode centred on some specific resonator, indexed by i_d .

The creation of a localised eigenmode occurs by modifying the wave speed inside the resonator i_d . This approach is particularly suited to a disordered system because it does not rely on any geometrical assumption. Mathematically, this translates to considering the eigenvalues of the generalised capacitance matrix $\mathcal{C} = VC$ with V instead of being defined as in (1.1) is now given by

$$V := \begin{pmatrix} \frac{v_1^2 \delta_1}{|D_1|} & & & & \\ & \ddots & & & \\ & & \frac{(v_{i_d} + \eta)^2 \delta_{i_d}}{|D_{i_d}|} & & \\ & & & \ddots & \\ & & & & \frac{v_N^2 \delta_N}{|D_N|} \end{pmatrix}.$$

In principle, there is no reason why this procedure should generate localised eigenmodes also for disordered systems, after all, there is no clear (periodic) structure that is perturbed. However, the underlying bandgap structure supports the presence of these eigenmodes.

In Figure 8, we show the result of this procedure on a structure composed of disordered blocks as in Figure 4(A). Two eigenvalues jump into the bandgap and their corresponding eigenmodes become localised around the index i_d at which the perturbation is performed. We note that the two eigenmodes have very different decay rates. As in periodic systems, this is due to the different distances that the two eigenvalues in the gap have from the bands.

4.1. Defect eigenmode prediction

The capacitance matrix approximation of the system delivers the following modal decomposition of the Green function $G(\omega)$ associated with the system of resonators:

$$G(\omega) = (\mathcal{C} - \omega^2 I_N)^{-1} = \sum_j \frac{u_j \bar{u}_j^\top}{\omega^2 - \lambda_j}, \quad (4.1)$$

for ω^2 not being an eigenvalue of \mathcal{C} , where I_N is the $N \times N$ identity matrix (with N being the number of resonators) and (λ_j, u_j) are the eigenpairs of \mathcal{C} .

Away from the spectrum of \mathcal{C} , we can thus predict the outline of the eigenmode associated with an excitation at the i^{th} resonator by $G(\omega)e_i$, where $(e_i)_{i=1}^N$ denotes the standard basis of \mathbb{R}^N . The absolute error in predicting the defect eigenmode v_d via $G(\omega_d)e_{i_d}$ is of the order of 10^{-13} with ω_d being the defect eigenfrequency. Remark that for this computation one can use the unperturbed generalised capacitance matrix providing an accurate *a priori* estimation of the defect eigenmodes. However, the defect eigenfrequency ω_d still needs to be computed.

The modal decomposition (4.1) can generally be used to show that, as in the periodic case, the defect midgap eigenvalues are associated with localised eigenmodes. This follows from the fact that the generalised capacitance matrix has entries that decay at least as the inverse of the distances between the resonators. Furthermore, by [31], when a nonsingular

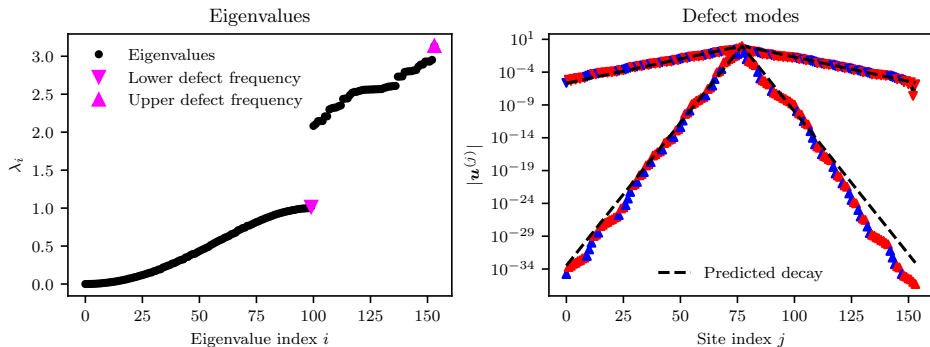


FIGURE 8. Defect modes for a disordered system as in Example 3.1 with $M = 100$ blocks and a defected dimer in the middle ($i_d = N/2, \eta = 0.2$). **Left:** Spectrum of the defected system with two defect frequencies in the bandgap. **Right:** The two eigenmodes corresponding to the defect frequencies. The upper / lower triangle marks correspond to the upper / lower defect frequency and the mark colour indicates whether the respective site belongs to a single resonator block (blue) or dimer block (red). The eigenmodes are exponentially localised about the defected site, with their rate of decay closely matching the predicted decay (dashed line) obtained by taking the expected decay in the blocks. The outline of the localised eigenvectors is effectively predicted by the discrete Green function of (4.1) up to an error of 10^{-13} .

matrix has geometrically decaying entries, then its inverse also has a similar decay with a possibly different rate.

At the beginning of this section, we have commented on the different decay rates of the defect eigenvectors showing in Figure 8. This effect turns out to have an interesting origin. In Figure 9 we show that the position of the defect eigenvalue depends on which of the blocks is chosen for the perturbation. Recall that we are considering a disordered block structure composed of two types of blocks — dimer blocks and monomer blocks — arranged in a random manner. In the left part of Figure 9 we see that if we perturb one of the single resonator blocks the upper defect eigenmode stays fixed while the lower defect eigenmode moves across the bandgap. For larger perturbations, the lower eigenmode ceases to move, and the upper defect eigenmode moves up instead. If we instead perturb a dimer block, we see the opposite picture. Perturbation causes the upper defect eigenmode to move into the upper gap while the lower defect eigenmode barely moves. We remark furthermore, that if one happens to know beforehand that the last eigenvalue of a band is a hybridised bound eigenfrequency with eigenmode localised around some resonator, then perturbing that precise resonator makes the eigenvalue immediately jump into the bandgap avoiding the initially flat part of the blue curve in Figure 9(B). Note that in Figure 8 we perturb a dimer block inducing a large jump for the upper defect eigenvalue and a small jump for the lower one. This is reflected in the two very different decay rates of the corresponding eigenmodes.

Once the defect frequency is known, we can employ the propagation matrix formalism to find precise defect rate predictions for block disordered systems. We denote $L_X(\omega) = \ln |\sigma_-(P_X(\omega^2))|$ the *Lyapunov exponent* at frequency ω where P_X denotes the total propagation matrix of the single resonator block $X = S$ or dimer block $X = D$, respectively, and $\sigma_-(\cdot)$ selects the eigenvalue with the lowest absolute value. We note that because $\det P_X = 1$ we must always have $L_X(\omega) \leq 0$.

Recall that the single resonator S is sampled with probability p_S and the dimer D with probability p_D . The decay of some defect mode with eigenfrequency ω after K random

blocks is thus given by the random variable

$$Y = e^{L_S(\omega)X} e^{L_D(\omega)(K-X)}, \quad (4.2)$$

where $X \sim \text{Bin}(p_S, K)$ is sampled from the binomial distribution. Therefore, the expected decay after K random blocks is given by

$$E[Y] = (p_S e^{L_S(\omega)} + p_D e^{L_D(\omega)})^K. \quad (4.3)$$

As we can see in Figure 8, this prediction matches the actual decay rate very closely. At this point, we note that this decay rate argument is also able to predict the decay of hybridised bound eigenmodes between sites of localisation as seen in Figure 7 but fails to account for the collocation induced by hybridisation. However, because defect modes only resonate at their defect site (in the case of a single defect) the decay prediction applies without any issue.

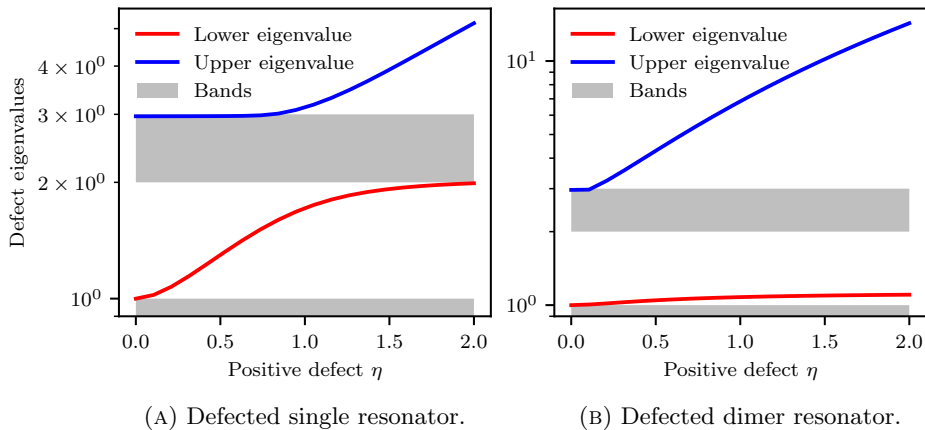


FIGURE 9. Defect eigenfrequency as a function of positive material parameter perturbation strength. We are perturbing the structure from Figure 4(A). Left: Perturbation of a single resonator block creating a large jump in the lower eigenvalue. Right: Perturbation of a dimer resonator block creating a large jump in the upper eigenvalue.

4.2. Dimer Defect

Another interesting effect recently observed in [8] for the periodic case is the *repulsion effect* occurring when two adjacent resonators are perturbed by the procedure illustrated at the beginning of the section. Level repulsion means that when randomness is added to the entries of a matrix, the eigenvalues tend to separate. In periodic systems, such a perturbation induces two coupled eigenmodes to jump into the bandgap and to be localised once with a dipole (odd) symmetry and once with a monopole (even) symmetry. We analyse this situation for disordered systems. In Figure 10 we plot the two largest eigenvalues when such a perturbation is performed observing the same level of repulsion seen in periodic structures.

5. Stability analysis

A natural question that arises when studying the bands and bandgaps of disordered systems is whether they are stable under perturbation.

To that end, in line with the previous section, we investigate the behaviour of our disordered systems as the wave speeds inside the resonators are perturbed globally. Recall that the spectra of these systems are described by the eigenvalues of VC where V is a diagonal matrix

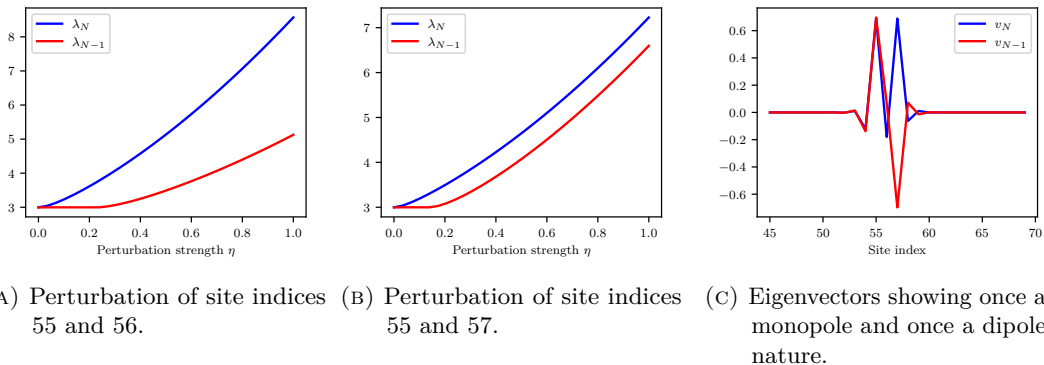


FIGURE 10. When perturbing juxtaposed resonators two eigenvalues jump into the bandgaps. The distance between these eigenvalues depends on the distance between the perturbed resonators. In any case, the eigenvectors display opposed nature.

encoding material parameters and sizes of the resonators, namely $V_{ii} = v_i^2 \delta_i / |D_i|$ and the entries of C depend only on the geometry of the resonators.

In the unperturbed case, all resonators have the same wave speed $v_i = 1$. We now globally perturb the wave speed as follows:

$$v'_i = v_i + \eta_i,$$

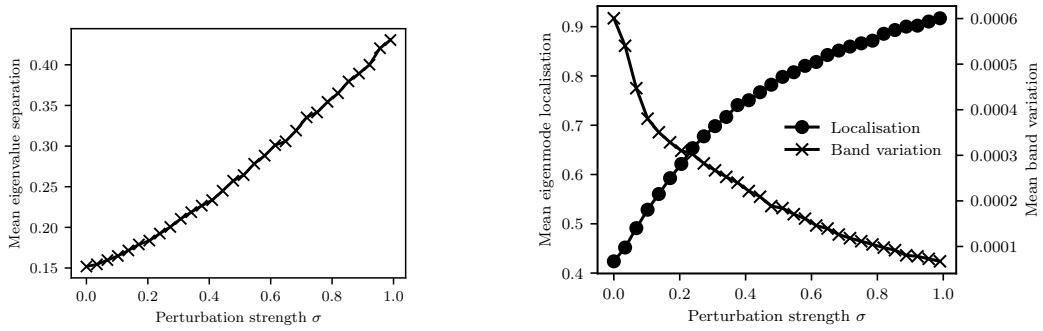
where the perturbations $\eta_i \sim \mathcal{U}[-\sigma, \sigma]$ are independently drawn from the uniform distribution $\mathcal{U}[-\sigma, \sigma]$ with support in $[-\sigma, \sigma]$. In particular, we note that such perturbations destroy the prior block structure of our disordered block systems.

This setup resembles the one found in [8] for the purely periodic case. Indeed, many observations from the periodic case still hold in the disordered bandgapped setting. Figure 11 demonstrates that the two statistical phenomena that dominate the periodic case continue to do so in the disordered case. Namely, level repulsion pushing the eigenvalues apart, as demonstrated by the increasing mean eigenvalue separation and Anderson localisation causing a complete localisation of the eigenmodes, as demonstrated by the decreasing mean band variation and increasing degree of localisation.

These two forces are illuminated further in Figure 12. The starting point is the disordered system with two pass bands introduced in Figure 4(A). Without perturbation, we can see that the density of eigenfrequencies is evenly distributed into the two bands, with slightly higher density at the band edges. For small perturbations the bandgap remains unaltered, this is due to Weyl's spectral stability result and the inherited Hermitian nature of the problem. As the perturbation strength increases, the band edges begin to dissolve as level repulsion causes the eigenvalues to spread out, causing a progressive closing of the bandgap. This also illustrates why the lower band is more resistant to perturbation, as the eigenvalues cannot spread out below zero. At the same time, Anderson localisation causes the eigenmodes to localise, where again the eigenmodes in the upper band are more susceptible. Furthermore, for large perturbation strength, the bandgap vanishes and the majority of eigenmodes become fully localised as the system transitions from a disordered but structured system to a fully random and unstructured one.

Finally, in Figure 13 we compare the perturbation response to the periodic dimer system. For all three systems, the observed behaviour mirrors the one observed in Figure 12 as the eigenvalues spread out and the eigenmodes become localised. In particular, the global perturbation seems to make no distinction between extended eigenmodes and hybridised bound eigenmodes, both becoming completely delocalised for large perturbation strengths.

The material parameter perturbation is general in the sense that both spacing and resonator size perturbations cause the same localisation behaviour. This is not surprising,



(A) Level Repulsion: Mean eigenvalue separation as a function of the perturbation strength σ .

(B) Anderson localisation: Mean eigenmode localisation $\|u\|_\infty / \|u\|_2$ and mean band variation as a function of the perturbation strength σ .

FIGURE 11. Level repulsion and Anderson localisation under material parameter perturbation (averaged over 100 random realisations). The material parameters of the double pass band system from Figure 4(B) are perturbed uniformly with perturbation strength σ .

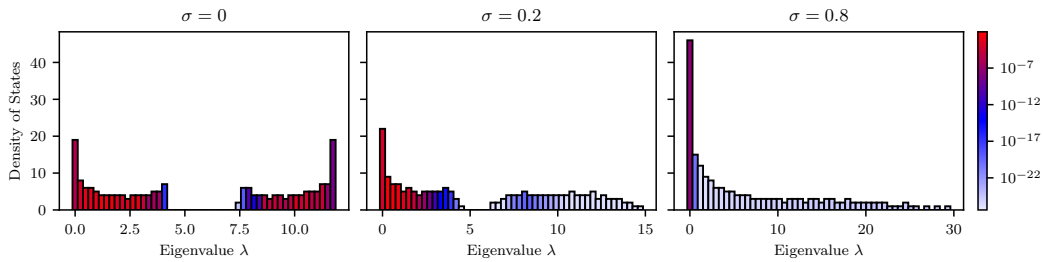


FIGURE 12. Density of eigenfrequencies and band variation under material parameter perturbation (averaged over 100 random realisations). We again perturb the double pass band system from Figure 4(B) uniformly. The colours mark the mean band variation in the corresponding bin. As the perturbation strength increases the density of eigenfrequencies spreads out, converging to the expected e^{-x} distribution [8] and the eigenmodes become localised.

given that perturbations in the material, spacing, and size of the resonators induce equivalent perturbations in the governing matrix VC .

6. Prediction of wave localisation positions and mobility edges

6.1. Landscape function for predicting wave localisation positions

In this section, we first consider the landscape function and compare its performance of the landscape function for the detection of localised eigenmodes in perturbed periodic systems with that in disordered systems when hybridised eigenmodes occur.

The landscape function first introduced in [25] has already been used to predict lwave ocalisation in subwavelength resonator systems [20]. The prediction is through the computation of the solution \mathbf{u} of

$$VC\mathbf{u} = \mathbf{1}, \quad (6.1)$$

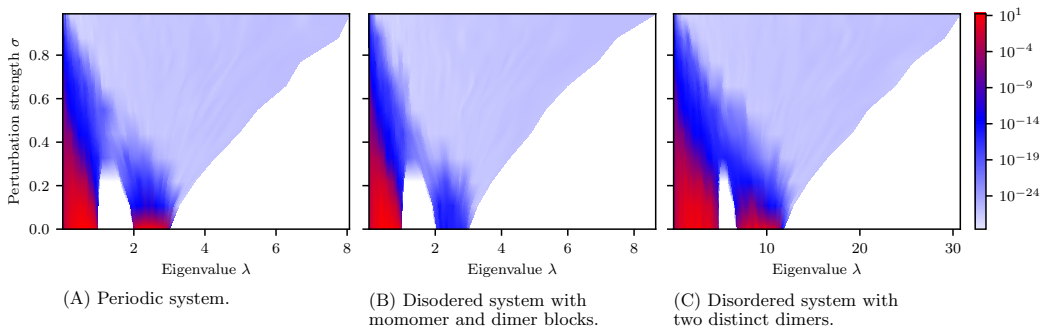
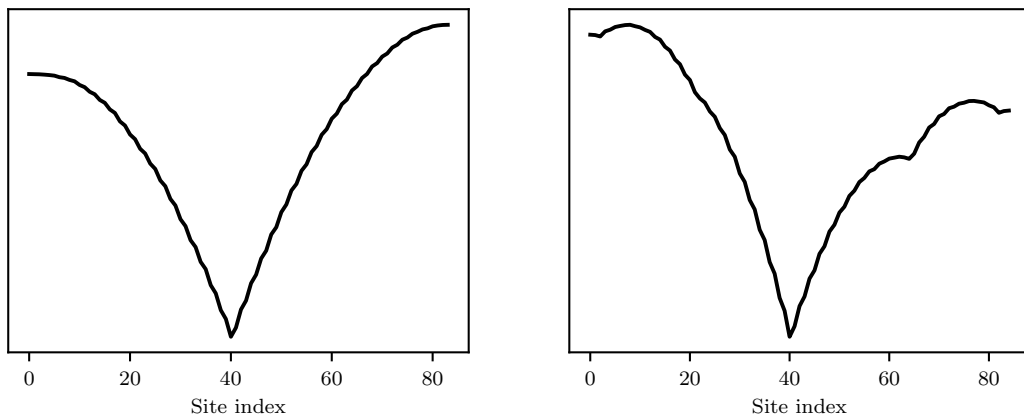


FIGURE 13. Band variation and spectral distribution of different systems under material parameter perturbation (averaged over 100 random realisations). We perturb the periodic dimer system from Figure 1(A) and the single and double pass band disordered systems from Figure 4(A and B) uniformly. The colours mark the band variation of the eigenmode at the corresponding point. The behaviour is the same in all cases, as the eigenvalues spread out and the corresponding eigenmodes become increasingly more localised.

where $\mathbf{1}$ is the vector of only ones. We note that generally in one dimension this procedure does not work if all resonators have the same material parameters, because of the singularity of C . Nevertheless, for defected systems as introduced in Section 4, it might be applied. In Figure 14, we show that the localisation landscape can also be used for the detection of localised eigenmodes even in the presence of hybridised bound eigenmodes. Comparing Figure 14(A) and Figure 14(B), we observe an increased noise level due to the hybridised bound eigenmodes. However, this effect is orders of magnitude smaller than the pattern induced by the defect material parameter.



(A) Periodic structure of dimers with material parameter defect at the site index 40. (B) Disordered structure with hybridised bound eigenmodes from Figure 4(A) with additional material parameter defect at the site index 40.

FIGURE 14. The landscape function predicts the localisation induced by material parameter defects in disordered systems even in the case when hybridised eigenmodes occur.

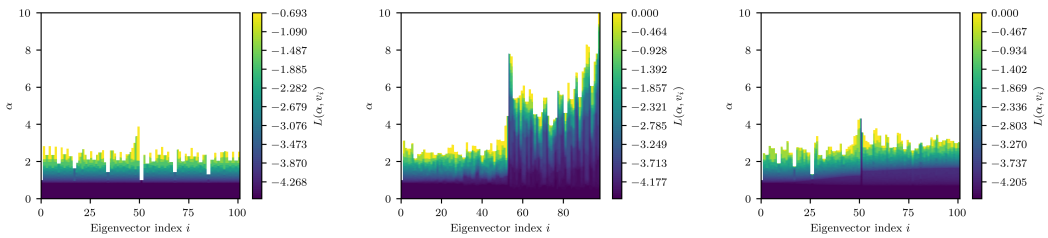
6.2. Fractal dimension of localised eigenmodes for predicting mobility edges

Finally, we show that the behaviour of the fractal dimension related the localised eigenmodes of randomly perturbed systems can be used to identify the mobility edges in disordered systems even when hybridised eigenmodes occur.

Specifically, in this framework, the fractal dimension of an eigenvector $v \in \mathbb{R}^N$ of the capacitance matrix C is defined as

$$L(\alpha, v) := -\ln(|\{i : v_i^2 < N^{-\alpha}\}|) \quad (6.2)$$

for $\alpha \in \mathbb{R}$; see, for instance, [17]. We remark two interesting values for L : $L(\alpha, \mathbf{1}/\|\mathbf{1}\|) = -\ln(N)$ for $\alpha < 1$ and undefined for $\alpha \geq 1$, and $L(\alpha, e_i) = -\ln(N)$ for every α where e_i is an element of the standard basis.



(A) Periodic structure.

(B) Disordered structure with hybridised bound eigenmodes from Figure 4(A) with material parameter defect at index 50.

(C) Periodic structure with single material parameter defect at index 50.

FIGURE 15. The fractal dimension shows a clear difference between locally translation invariant structures and disordered structures. A clear phase change between the delocalised and the hybridised bound eigenmodes can be observed in (B).

As shown in Figure 15, the fractal dimension indicates a clear phase change when moving from delocalised to hybridised bound eigenmodes in Figure 15(B). Here, two observations are in order. On the one hand, the fractal dimension of the delocalised states is qualitatively indistinguishable from the one of a periodic structure. On the other hand, the bound states show a much richer fractal dimension and the two localised states induced by the material parameter defect stick out — as in Figure 15(c) — by having the lowest fractal dimension.

The periodic case in Figure 15(A) and the defected structure in Figure 15(c) behave similarly except for the localised eigenmode in the latter.

7. Concluding remarks

In this paper, we have shown how to extend the mechanism of subwavelength localisation under random perturbation of the material parameter from periodic systems of resonators to spatially disordered systems of resonators. By imposing quasiperiodic boundary conditions on the disordered system, we have introduced natural generalisations of the notions of bandgap, mobility edge, and midgap defect eigenmode. We have also introduced a localised eigenmode prediction based on the discrete Green function of the disordered system of resonators. We have observed the existence of hybridised bound eigenmodes in structures where local translation invariance is broken. In systems consisting of a random resonator block array, the necessary condition for the occurrence of such hybridised bound eigenmodes is that the bandgaps of the constituent resonator blocks are not identical. Only eigenvalues in the overlap of all bandgaps correspond to localised eigenmodes whereas eigenvalues in some of the bandgaps but not in all correspond to hybridised bound eigenmodes. Finally, we have

shown that both the landscape function and the fractal dimension of eigenvectors of the capacitance matrix can be applied to detect, respectively, localised eigenmodes and mobility edges in disordered structures even in the presence of hybridised eigenmodes.

On the one hand, our results in this paper open the door to the study of wave localisation in other classes of disordered structures such as quasiperiodic or hyperuniform ones (see, for instance, [21, 47]) as well as in non-Hermitian systems of subwavelength resonators with gauge potentials [2, 3, 27, 43, 49, 50]. On the other hand, our findings here motivate the study of the distributions of the eigenvalues and the localisation properties of the eigenvectors of products of two matrices; one is a diagonal matrix with independent randomly perturbed entries and the other is an M-matrix. The study of random M-matrices with correlated entries would also be of great interest in wave physics in the subwavelength regime. In general, little is known about the statistical properties of eigenvalues and eigenvectors of random matrices whose entries are correlated.

Acknowledgments

The work of AU was supported by the Swiss National Science Foundation grant number 200021–200307. The authors thank Bryn Davies, Erik Hiltunen, Antti Knowles, Ping Liu, and Svitlana Mayboroda for insightful discussions.

Code availability

The software used to produce the numerical results in this work is openly available at <https://doi.org/10.5281/zenodo.14383676>.

References

- [1] AIZENMAN Michael and MOLCHANOV Stanislav, “Localization at large disorder and at extreme energies: an elementary derivation”, in: *Comm. Math. Phys.* 157.2 (1993), pp. 245–278.
- [2] AMMARI Habib, BARANDUN Silvio, CAO Jinghao, DAVIES Bryn, and HILTUNEN Erik Orvehed, “Mathematical Foundations of the Non-Hermitian Skin Effect”, in: *Arch. Rational Mech. Anal.* 248.3 (2024), p. 33.
- [3] AMMARI Habib, BARANDUN Silvio, CAO Jinghao, DAVIES Bryn, HILTUNEN Erik Orvehed, and LIU Ping, “The Non-Hermitian Skin Effect With Three-Dimensional Long-Range Coupling”, in: *J. Eur. Math. Soc. (JEMS)*, to appear (2025).
- [4] AMMARI Habib, BARANDUN Silvio, CAO Jinghao, and FEPPON Florian, “Edge Modes in Subwavelength Resonators in One Dimension”, in: *Multiscale Model. Simul.* 21.3 (2023).
- [5] AMMARI Habib, BARANDUN Silvio, DAVIES Bryn, HILTUNEN Erik Orvehed, KOSCHE Thea, and LIU Ping, “Exponentially Localized Interface Eigenmodes in Finite Chains of Resonators”, in: *Stud. Appl. Math.* 153.4 (2024), Paper No. e12765, 25.
- [6] AMMARI Habib, BARANDUN Silvio, LIU Ping, and UHLMANN Alexander, *Tunable Localisation in Parity-Time-Symmetric Resonator Arrays with Imaginary Gauge Potentials*, version 1, 2024, DOI: 10.48550/ARXIV.2405.05002, pre-published.
- [7] AMMARI Habib, BARANDUN Silvio, and UHLMANN Alexander, *Truncated Floquet-Bloch transform for computing the spectral properties of large finite systems of resonators*, 2024, arXiv: 2410.17597.
- [8] AMMARI Habib, DAVIES Bryn, and HILTUNEN Erik Orvehed, “Anderson Localization in the Subwavelength Regime”, in: *Commun. Math. Phys.* 405.1 (2024), p. 1.
- [9] AMMARI Habib, DAVIES Bryn, and HILTUNEN Erik Orvehed, “Convergence rates for defect modes in large finite resonator arrays”, in: *SIAM J. Math. Anal.* 55.6 (2023), pp. 7616–7634.
- [10] AMMARI Habib, DAVIES Bryn, and HILTUNEN Erik Orvehed, “Functional Analytic Methods for Discrete Approximations of Subwavelength Resonator Systems”, in: *Pure Appl. Anal.* 6.3 (2024), pp. 873–939.

- [11] AMMARI Habib, DAVIES Bryn, and HILTUNEN Erik Orvehed, *Mathematical theories for metamaterials: From condensed matter theory to subwavelength physics*, NSF–CBMS Regional Conf. Ser. American Mathematical Society, Providence, to appear, 2024.
- [12] AMMARI Habib, DAVIES Bryn, and HILTUNEN Erik Orvehed, “Robust Edge Modes in Dislocated Systems of Subwavelength Resonators”, in: *J. London Math. Soc.* 106.3 (Apr. 2022), pp. 2075–2135.
- [13] AMMARI Habib, DAVIES Bryn, and HILTUNEN Erik Orvehed, “Spectral Convergence in Large Finite Resonator Arrays: The Essential Spectrum and Band Structure”, in: *Bulletin London Math. Soc.*, to appear (2024), DOI: <https://doi.org/10.1112/blms.13225>.
- [14] AMMARI Habib, FITZPATRICK Brian, GONTIER David, LEE Hyundae, and ZHANG Hai, “Minnaert Resonances for Acoustic Waves in Bubbly Media”, in: *Ann. Inst. H. Poincaré C Anal. Non Linéaire* 35.7 (2018), pp. 1975–1998.
- [15] AMMARI Habib, FITZPATRICK Brian, LEE Hyundae, YU Sanghyeon, and ZHANG Hai, “Subwavelength phononic bandgap opening in bubbly media”, in: *J. Differential Equations* 263.9 (2017), pp. 5610–5629.
- [16] ARNOLD Douglas, FILOCHE Marcel, MAYBORODA Svitlana, WANG Wei, and ZHANG Shiwen, “The Landscape Law for Tight Binding Hamiltonians”, in: *Commun. Math. Phys.* 396.3 (2022), pp. 1339–1391.
- [17] BARBER Enrique Maciá, *Aperiodic structures in condensed matter*, Series in Condensed Matter Physics, Fundamentals and applications, CRC Press, Boca Raton, FL, 2009.
- [18] CHEBEN Pavel, HALIR Robert, SCHMID Jens H., ATWATER Harry A., and SMITH David R., “Subwavelength integrated photonics”, in: *Nature* 560 (2018), pp. 565–572.
- [19] CUMMER Steven A., CRISTENSEN Johan, and ALÙ Andrea, “Controlling sound with acoustic metamaterials”, in: *Nature Rev. Mater.* 1.3 (2016), p. 16001.
- [20] DAVIES Bryn and LOU Yiqi, “Landscape of Wave Focusing and Localization at Low Frequencies”, in: *Stud. Appl. Math.* 152.2 (2023), pp. 760–777.
- [21] DAVIES Bryn and MORINI Lorenzo, “Super band gaps and periodic approximants of generalised Fibonacci tilings”, in: *Proc. A.* 480.2285 (2024), Paper No. 20230663, 25.
- [22] DEAN P. and BACON M. D., “The Nature of Vibrational Modes in Disordered Systems”, in: *Proceedings of the Physical Society* 81.4 (Apr. 1963), p. 642, DOI: 10.1088/0370-1328/81/4/305, (visited on 01/13/2025).
- [23] EDWARDS J.T. and THOULESS D.J., “Numerical studies of localization in disordered systems”, in: *J. Phys. C: Solid State Phys.* 5 (1972), pp. 807–820.
- [24] FEPPON Florian, CHENG Zijian, and AMMARI Habib, “Subwavelength Resonances in One-Dimensional High-Contrast Acoustic Media”, in: *SIAM J. Appl. Math.* 83.2 (2023), pp. 625–665.
- [25] FILOCHE Marcel and MAYBORODA Svitlana, “Universal mechanism for Anderson and weak localization”, in: *Proc. Natl. Acad. Sci. USA* 109.37 (2012), pp. 14761–14766.
- [26] FILOCHE Marcel, MAYBORODA Svitlana, and TAO Terence, “The effective potential of an M -matrix”, in: *J. Math. Phys.* 62.4 (2021), Paper No. 041902, 15.
- [27] HATANO Naomichi and NELSON David R., “Localization Transitions in Non-Hermitian Quantum Mechanics”, in: *Physical Review Letters* 77.3 (July 1996), pp. 570–573, DOI: 10.1103/PhysRevLett.77.570.
- [28] HISLOP Peter D., “Lectures on random Schrödinger operators”, in: *Fourth Summer School in Analysis and Mathematical Physics*, vol. 476, Contemp. Math. Amer. Math. Soc., Providence, RI, 2008, pp. 41–131.
- [29] HORI J.-i. and MATSUDA H., “Structure of the Spectra of Disordered Systems. I”, in: *Prog. Theor. Phys.* 32.2 (1964), pp. 183–189.
- [30] HORI Jun-ichi, “Structure of the Spectra of Disordered Systems. II: Spectral Gaps of Disordered Systems”, in: *Prog. Theor. Phys.* 32.3 (1964), pp. 371–379.
- [31] JAFFARD S., “Propriétés des matrices “bien localisées” près de leur diagonale et quelques applications”, in: *Ann. Inst. H. Poincaré C Anal. Non Linéaire* 7.5 (1990), pp. 461–476.

- [32] KADIC Muamer, MILTON Graeme W., HECKE Martin van, and WEGENER Martin, “3D metamaterials”, in: *Nature Rev. Phys.* 1 (3 2019), pp. 2522–5820.
- [33] LEMOULT Fabrice, FINK Mathias, and LEROSEY Geoffroy, “Acoustic Resonators for Far-Field Control of Sound on a Subwavelength Scale”, in: *Phys. Rev. Lett.* 107.6 (2011), p. 064301.
- [34] LEMOULT Fabrice, KAINA Nadège, FINK Mathias, and LEROSEY Geoffroy, “Soda Cans Metamaterial: A Subwavelength-Scaled Phononic Crystal”, in: *Crystals* 6.7 (2016).
- [35] LIU Zhengyou, ZHANG Xixiang, MAO Yiwei, ZHU Y. Y., YANG Zhiyu, CHAN C. T., and SHENG Ping, “Locally Resonant Sonic Materials”, in: *Science* 289 (5485 2000), pp. 1734–1736.
- [36] LYRA M. L., MAYBORODA S., and FILOCHE M., “Dual Landscapes in Anderson Localization on Discrete Lattices”, in: *EPL (Europhysics Letters)* 109.4 (2015), p. 47001.
- [37] MA G. and SHENG P., “Acoustic metamaterials: From local resonances to broad horizons”, in: *Science Advances* 2.2 (2016), 2:e1501595.
- [38] MINAMI Nariyuki, “Local fluctuation of the spectrum of a multidimensional Anderson tight binding model”, in: *Comm. Math. Phys.* 177.3 (1996), pp. 709–725.
- [39] MINNAERT M., “On musical air-bubbles and the sounds of running water”, in: *Philos. Mag.* 16.104 (1933), pp. 235–248.
- [40] MOLCANOV S.A., “The Local Structure of the Spectrum of the One-Dimensional Schrödinger Operator”, in: *Comm. Math. Phys.* 78.3 (1981), pp. 429–446.
- [41] PLEMMONS R. J., “ M -matrix characterizations. I. Nonsingular M -matrices”, in: *Linear Algebra Appl.* 18.2 (1977), pp. 175–188.
- [42] POOLE George and BOULLION Thomas, “A survey on M -matrices”, in: *SIAM Rev.* 16 (1974), pp. 419–427.
- [43] RIVERO Jose H. D., FENG Liang, and GE Li, “Imaginary Gauge Transformation in Momentum Space and Dirac Exceptional Point”, in: *Physical Review Letters* 129.24 (Dec. 2022), p. 243901, DOI: 10.1103/PhysRevLett.129.243901.
- [44] SAXON D. S. and HUTNER R. A., “Some electronic properties of a one-dimensional crystal model”, in: *Philips J. Res.* 4 (1949), pp. 81–122.
- [45] THOULESS D J, “A Relation between the Density of States and Range of Localization for One Dimensional Random Systems”, in: *J. Phys. C: Solid State Phys.* 5.1 (1972), p. 77.
- [46] THOULESS D.J., “Electrons in Disordered Systems and the Theory of Localization”, in: *Phys. Rep.* 13.3 (1974), pp. 93–142.
- [47] TORQUATO Salvatore, “Hyperuniform states of matter”, in: *Phys. Rep.* 745 (2018), pp. 1–95.
- [48] WINDISCH Günther, *M-matrices in numerical analysis*, vol. 115, Teubner-Texte zur Mathematik [Teubner Texts in Mathematics], With German, French and Russian summaries, BSB B. G. Teubner Verlagsgesellschaft, Leipzig, 1989.
- [49] YAO Shunyu and WANG Zhong, “Edge States and Topological Invariants of Non-Hermitian Systems”, in: *Physical Review Letters* 121.8 (Aug. 2018), DOI: 10.1103/physrevlett.121.086803.
- [50] YOKOMIZO Kazuki, YODA Taiki, and MURAKAMI Shuichi, “Non-Hermitian Waves in a Continuous Periodic Model and Application to Photonic Crystals”, in: *Phys. Rev. Res.* 4.2 (May 2022), p. 023089, DOI: 10.1103/PhysRevResearch.4.023089.
- [51] YVES Simon, FLEURY Romain, BERTHELOT Thomas, FINK Mathias, LEMOULT Fabrice, and LEROSEY Geoffroy, “Crystalline Metamaterials for Topological Properties at Subwavelength Scales”, in: *Nat. Commun.* 8.1 (2017), p. 16023.

REFERENCES

HABIB AMMARI

ETH ZÜRICH, DEPARTMENT OF MATHEMATICS, RÄMISTRASSE 101, 8092 ZÜRICH, SWITZERLAND,
ORCID.ORG/0000-0001-7278-4877

Email address: habib.ammari@math.ethz.ch

SILVIO BARANDUN

ETH ZÜRICH, DEPARTMENT OF MATHEMATICS, RÄMISTRASSE 101, 8092 ZÜRICH, SWITZERLAND,
ORCID.ORG/0000-0003-1499-4352

Email address: silvio.barandun@sam.math.ethz.ch

ALEXANDER UHLMANN

ETH ZÜRICH, DEPARTMENT OF MATHEMATICS, RÄMISTRASSE 101, 8092 ZÜRICH, SWITZERLAND,
ORCID.ORG/0009-0002-0426-6407

Email address: alexander.uhlmann@sam.math.ethz.ch